The Astrophysical Journal, 797:107 (8pp), 2014 December 20 doi:10.1088/0004-637X/797/2/107

RELATIVISTIC SUPERNOVAE HAVE SHORTER-LIVED CENTRAL ENGINES OR MORE EXTENDED PROGENITORS: THE CASE OF SN 2012ap

R. Margutti[1], D. Milisavljevic[1], A. M. Soderberg[1], C. Guidorzi[2], B. J. Morsony[3], N. Sanders[1], S. Chakraborti[1], A. Ray[4], A. Kamble[1], M. Drout[1], J. Parrent[1], A. Zauderer[1], and L. Chomiuk[5]
[1] Harvard-Smithsonian Center for Astrophysics, 60 Garden Street, Cambridge, MA 02138, USA
[2] Department of Physics and Earth Sciences, University of Ferrara, via Saragat 1, I-44122 Ferrara, Italy
[3] Department of Astronomy, University of Wisconsin-Madison, 2535 Sterling Hall, 475 North Charter Street, Madison, WI 53706-1582, USA
[4] Department of Astronomy and Astrophysics, Tata Institute of Fundamental Research, 1 Homi Bhabha Road, Mumbai 400 005, India
[5] Department of Physics and Astronomy, Michigan State University, East Lansing, MI 48824, USA
Received 2014 February 12; accepted 2014 October 14; published 2014 December 5

ABSTRACT

Deep, late-time X-ray observations of the relativistic, engine-driven, type Ic SN 2012ap allow us to probe the nearby environment of the explosion and reveal the unique properties of relativistic supernova explosions (SNe). We find that on a local scale of ∼0.01 pc the environment was shaped directly by the evolution of the progenitor star with a pre-explosion mass-loss rate of $\dot{M} < 5 \times 10^{-6}\, M_{\odot}\, \mathrm{yr}^{-1}$, in line with gamma-ray bursts (GRBs) and the other relativistic SN 2009bb. Like sub-energetic GRBs, SN 2012ap is characterized by a bright radio emission and evidence for mildly relativistic ejecta. However, its late-time ($\delta t \approx 20$ days) X-ray emission is ∼100 times fainter than the faintest sub-energetic GRB at the same epoch, with no evidence for late-time central engine activity. These results support theoretical proposals that link relativistic SNe like 2009bb and 2012ap with the weakest observed engine-driven explosions, where the jet barely fails to break out. Furthermore, our observations demonstrate that the difference between relativistic SNe and sub-energetic GRBs is intrinsic and not due to line-of-sight effects. This phenomenology can either be due to an intrinsically shorter-lived engine or to a more extended progenitor in relativistic SNe.

Key words: gamma-ray burst: general – supernovae: individual (SN 2012ap)

Online-only material: color figures

1. INTRODUCTION

The vast majority of supernova explosions (SNe) arising from hydrogen- and helium-stripped progenitors (i.e., type Ic SNe; see Filippenko 1997 for the spectral classification of SNe) can be explained by the hydrodynamical collapse of the massive progenitor star (e.g., Tan et al. 2001). In a very limited percentage of cases ($\lesssim$1%; Berger et al. 2003; Coward 2005; Guetta & Della Valle 2007; Soderberg et al. 2010b), the explosion is instead powered by an engine able to accelerate a tiny portion of the ejecta with typical mass[6] $M \approx 10^{-5}$–$10^{-6}\, M_{\odot}$ to velocities $v \gtrsim 0.6\, c$. Engine-driven explosions (hereafter E-SNe) are thus uncommon. Furthermore, only a small fraction of E-SNe ($\lesssim$10%; e.g., Soderberg et al. 2006a; see also Cobb et al. 2006; Pian et al. 2006; Liang et al. 2007; Virgili et al. 2009) harbor a fully relativistic jet and give origin to gamma-ray bursts (GRBs). The peculiar circumstances that cause a hydrogen-stripped, massive progenitor star to produce a relativistic jet at the time of the collapse are still not fully understood. High angular momentum seems to be a key ingredient (e.g., MacFadyen & Woosley 1999; MacFadyen et al. 2001; Woosley & Heger 2006; Dessart et al. 2008).

E-SNe have historically been detected through their prompt X-ray and γ-ray emission produced by energy dissipation within the jet (ordinary GRBs) and by the SN shock break out (which is relevant at least for some sub-energetic, sub-E, GRBs; e.g., Kulkarni et al. 1998; Matzner & McKee 1999; MacFadyen et al. 2001; Tan et al. 2001; Campana et al. 2006; Wang et al. 2007; Waxman et al. 2007; Katz et al. 2010; Bromberg et al. 2011; Nakar & Sari 2012). More recently, two E-SNe have been discovered through their bright later-time radio emission (i.e., the relativistic SNe 2009bb and 2012ap; Soderberg et al. 2010b; Bietenholz et al. 2010; Chakraborti et al. 2011; Chakraborti et al. 2014, hereafter C14). Here, we specifically ask the following questions. What is the nature of relativistic SNe, and what is their connection with the other classes of E-SNe known so far?

The two known relativistic SNe 2009bb and 2012ap share with sub-E GRBs evidence for mildly relativistic ejecta powering a bright radio emission (Soderberg et al. 2006a, 2010b; Bietenholz et al. 2010; C14) and a very energetic optical explosion with $E_{\rm k} \sim 10^{52}$ erg coupled to material moving at $v \sim$ a few 10^4 km s^{-1} (Pignata et al. 2011; Milisavljevic et al. 2014b). These properties dynamically distinguish relativistic SNe and sub-E GRBs from ordinary SNe and put these explosions between the highly relativistic, collimated GRBs and the more common type Ic SNe.

On the theoretical side, state-of-the art simulations of jet-driven stellar explosions (e.g., Lazzati et al. 2012) associate classic GRBs with fully developed, highly relativistic jets and suggest that sub-E GRBs likely represent the cases where the jet is just barely able to pierce through the stellar envelope (Bromberg et al. 2011; Nakar & Sari 2012). In particular, it was suggested by Lazzati et al. 2012 that a different lifetime of the central engine might be able to explain the entire zoo of E-SNe (i.e., relativistic SNe, sub-E GRBs, and ordinary GRBs). However, it is unclear if relativistic SNe represent a new class of explosions, or if, instead, they are the equivalent of sub-E GRBs for which we missed the high-energy trigger because of line-of-sight effects or incomplete coverage of the γ-ray satellites (see, e.g., the discussion for SN 2009bb in Soderberg et al. 2010b). This still open question motivates this study.

[6] For the relativistic SN 2009bb, $M \approx 10^{-2}\, M_{\odot}$ (Chakraborti & Ray 2011).

We present late-time, deep X-ray observations of the relativistic SN 2012ap. These observations allow us to identify for the first time a distinctive property of relativistic SNe that clearly sets them apart from all the other known engine-driven explosions. We find that relativistic SNe are characterized by a significantly fainter X-ray emission at late times ($t \sim 20$ days), even compared to sub-E GRBs (SN 2012ap is $\sim$100 times fainter than the faintest sub-E GRB at the same epoch), and show no evidence for an excess of X-ray radiation that has been recently reported for the sub-E GRBs 060218 (Soderberg et al. 2006a; Fan & Piran 2006) and 100316D (Margutti et al. 2013a).

We describe our observations in Section 2 and constrain the progenitor mass-loss rate in Section 3. Finally, we put SN 2012ap in the context of engine-driven explosions in Sections 4 and 5 and discuss how our findings clearly suggest that relativistic SNe constitute a separate class of engine-driven explosions with intrinsic differences with respect to sub-E GRBs. Conclusions are drawn in Section 6.

Uncertainties are quoted at the 1σ confidence level, unless otherwise noted. We employ standard cosmology with $H_0 = 71\,\mathrm{km\,s^{-1}\,Mpc^{-1}}$, $\Omega_\Lambda = 0.73$, and $\Omega_\mathrm{M} = 0.27$. Throughout the paper, we use 2012 February 5 as the explosion date of SN 2012ap, as inferred by Milisavljevic et al. (2014b), hereafter M14) from extensive optical observations. Following C14, we assume a distance of 40 Mpc (Springob et al. 2007, 2009). A detailed discussion of the optical and radio properties of SN 2012ap can be found in M14 and C14, respectively. Finally, we note that sub-E GRBs are also called low-luminosity GRBs in the literature (see, e.g., Bromberg et al. 2011). However, the physical parameter that is relevant to your analysis is the (modest) kinetic energy of their fastest ejecta, which is surely related to the low luminosity of their prompt γ-ray emission. For this reason, we will refer to this class as sub-E GRBs.

2. OBSERVATIONS AND DATA ANALYSIS

2.1. Swift-XRT

We observed SN 2012ap with the *Swift* (Gehrels et al. 2004) X-ray Telescope (XRT; Burrows et al. 2005) starting from 2012 February 12 ($\delta t \approx 7$ days) until March 2 ($\delta t \approx 26$ d). No X-ray source is detected at the position of SN 2012ap. Analyzing the XRT data using the latest HEAsoft release (v6.13) and employing standard filtering and screening criteria, we determine a 3σ count-rate upper limit to the X-ray emission from SN 2012ap of 7.3×10^{-4} cps (0.3–10 keV energy band, total exposure time of 35 ks). The Galactic neutral hydrogen column density in the direction of SN 2012ap is $\mathrm{NH} = 4.9 \times 10^{20}\,\mathrm{cm^{-2}}$ (Kalberla et al. 2005). The analysis of the optical spectra presented in Milisavljevic et al. (2014a) constrains the intrinsic color excess toward SN 2012ap to be $0.18\,\mathrm{mag} < \mathrm{E(B-V)} < 0.57\,\mathrm{mag}$. Using the Galactic relations between the extinction A_V and the NH ($\mathrm{NH/A_V} \approx (1.7\text{–}2.2) \times 10^{21}\,\mathrm{cm^{-2}}$; Predehl & Schmitt 1995; Watson 2011), the limit on the color excess above translates into an intrinsic neutral hydrogen column density $\mathrm{NH_{x,i}} < 3.9 \times 10^{21}\,\mathrm{cm^{-2}}$. Assuming a simple power-law spectral model with photon index $\Gamma = 2$, the absorbed (unabsorbed) flux limit is $F_\mathrm{x} < 2.6 \times 10^{-14}\,\mathrm{erg\,s^{-1}cm^{-2}}$ ($F_\mathrm{x} < 5.8 \times 10^{-14}\,\mathrm{erg\,s^{-1}cm^{-2}}$), corresponding to a luminosity $L_\mathrm{x} < 1.1 \times 10^{40}\,\mathrm{erg\,s^{-1}}$ (0.3–10 keV) at a distance of 40 Mpc.

2.2. Chandra

We initiated deep X-ray follow-up of SN 2012ap with the *Chandra* X-ray Observatory on 2012 February 29.2 UT, $\delta t \approx 24$ days after the explosion (Program 13500648; PI: Soderberg). *Chandra* ACIS-S data were reduced with the `CIAO` software package (v4.5) and relative calibration files, applying standard ACIS data filtering. Using `wavedetect`, we find no evidence for X-ray emission at the position of SN 2012ap (Figure 1), with a 3σ limit of 8.0×10^{-4}cps (0.5–8 keV energy range, total exposure time of 9.9 ks). Employing the spectral parameters above, the corresponding absorbed (unabsorbed) flux limit in the 0.3–10 keV energy range is $F_\mathrm{x} < 6.8 \times 10^{-15}\,\mathrm{erg\,s^{-1}cm^{-2}}$ ($F_\mathrm{x} < 1.3 \times 10^{-14}\,\mathrm{erg\,s^{-1}cm^{-2}}$). The luminosity limit is $L_\mathrm{x} < 2.4 \times 10^{39}\,\mathrm{erg\,s^{-1}}$ (0.3–10 keV).

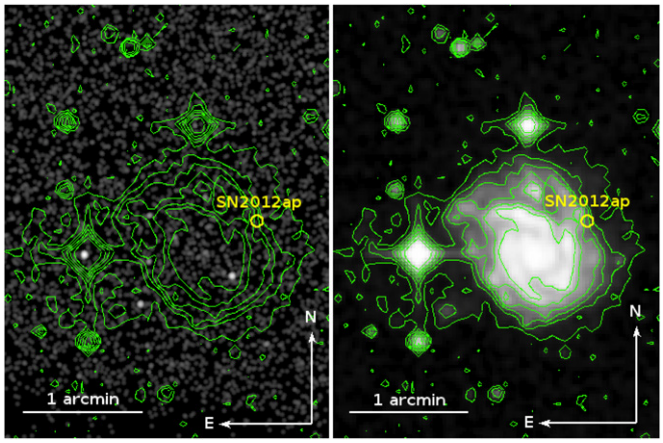

Figure 1. X-ray (*Chandra*, 0.5–8 keV; left panel) and pre-explosion optical image (SDSS; right panel) of the region around SN 2012ap. No X-ray emission is detected at the position of SN 2012ap at $\delta t \approx 24$ days after the explosion down to a deep luminosity limit of $L_\mathrm{x} \sim 2 \times 10^{39}\,\mathrm{erg\,s^{-1}}$ (0.3–10 keV). Yellow circle: 2″ radius region around SN 2012ap. Optical contours have been overlaid to the X-ray image for reference.

(A color version of this figure is available in the online journal.)

3. CONSTRAINTS ON THE PROGENITOR MASS-LOSS RATE

At $\delta t \lesssim 30$ days, inverse Compton (IC) is the dominating X-ray emission mechanism for ordinary SNe arising from hydrogen-stripped progenitors exploding in low-density environments (Björnsson & Fransson 2004; Chevalier & Fransson 2006). In the case of central-engine-powered SNe, additional sources of X-ray power are represented by continued central engine activity (as in the case of sub-E GRBs like 100316D; Margutti et al. 2013a) and interaction of the explosion jet with the environment (as in the case of ordinary GRBs; see, e.g., Margutti et al. 2013b). In the following, we use the deep *Chandra* limit of Section 2.2 and conservatively assume that IC is responsible for the entire X-ray emission to derive a solid upper limit to the mass-loss rate of the progenitor star of SN 2012ap.

In the IC scenario, the X-ray emission is originated by the up-scattering of optical photons from the SN photosphere by a population of relativistic electrons and depends on the density structure (1) of the SN ejecta and (2) of the circumstellar medium (CSM); (3) the details of the electron distribution responsible for the up-scattering; (4) the explosion parameters (ejecta mass M_ej and kinetic energy[7] E_k); and (5) the bolometric luminosity of the SN: $L_\mathrm{IC} \propto L_\mathrm{bol}$. We adopt the formalism by Margutti et al. (2012) modified to account for the outer density structure of SNe with compact progenitors that has been shown to scale

[7] This is the kinetic energy carried by the slowly moving material powering the optical emission.

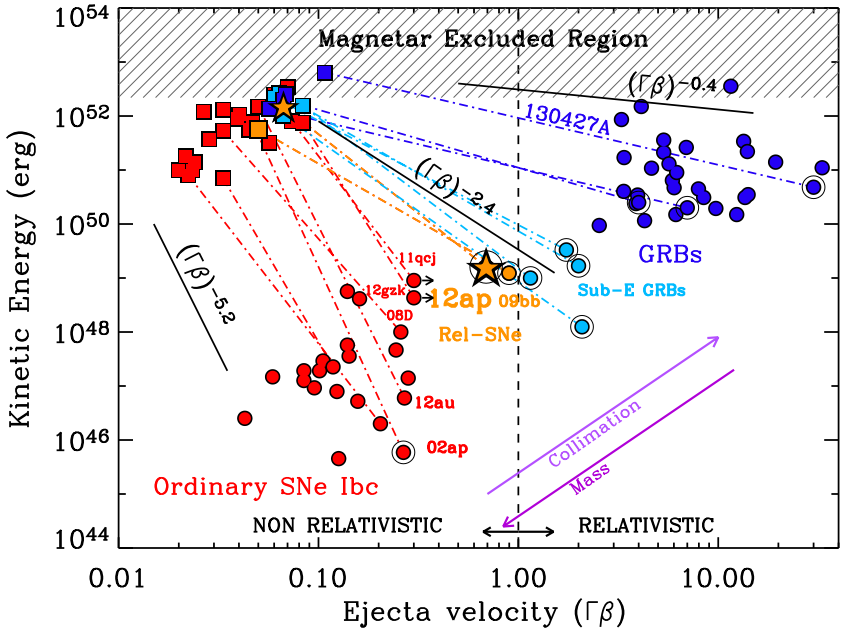

Figure 2. Kinetic energy profile of the ejecta of ordinary type Ibc SNe (red) and E-SNe, a class of explosions that includes GRBs (blue), sub-E GRBs (light-blue), and relativistic SNe (orange). Squares and circles are used for the slow-moving and the fast-moving ejecta, respectively, as measured from optical and radio observations. The velocity of the fast-moving ejecta has been computed at $\delta t = 1$ day (rest-frame). Black solid lines: ejecta kinetic energy profile of a pure hydrodynamical explosion ($E_{\rm k} \propto (\Gamma\beta)^{-5.2}$; Tan et al. 2001) and for explosions powered by a short-lived ($E_{\rm k} \propto (\Gamma\beta)^{-2.4}$) and long-lived ($E_{\rm k} \propto (\Gamma\beta)^{-0.4}$) central engine (Lazzati et al. 2012). Open black circles identify explosions with broad-lined optical spectra. The purple arrows identify the directions of increasing collimation and mass of the fastest ejecta. SN 2012ap bridges the gap between cosmological GRBs and ordinary SNe Ibc. Its kinetic energy profile, significantly flatter than what was expected from a pure hydrodynamical explosion, indicates the presence of a central engine (Margutti et al. (2013a), and references therein; Ben-Ami et al. (2012); Horesh et al. (2013); Corsi et al. (2014); Walker et al. (2014); C14; M14.

(A color version of this figure is available in the online journal.)

as $\rho_{\rm SN} \propto R^{-n}$ with $n \sim 10$ (see, e.g., Matzner & McKee 1999; Chevalier & Fransson 2006).

Assuming a wind-like CSM structure $\rho_{\rm CSM} \propto R^{-2}$ as appropriate for massive stars, a power-law electron distribution $n_e(\gamma) = n_0 \gamma^{-p}$ with $p \sim 3$ as indicated by radio observations of type Ib/c SNe (Chevalier & Fransson 2006) and by radio observations of SN 2012ap (C14), and a fraction of energy into relativistic electrons $\epsilon_e = 0.1$ as supported by well-studied SN shocks (e.g., Chevalier & Fransson 2006), the *Chandra* non-detection of SN 2012ap at $\delta t \approx 24$ days implies $\dot{M}/v_w < 5 \times 10^{-6} (M_\odot\,{\rm y}^{-1}/1000\,{\rm km\,s}^{-1})$. $\dot{M}$ is the mass-loss rate of the progenitor star, and v_w is the wind velocity. We renormalize the mass loss to $v_w = 1000\,{\rm km\,s}^{-1}$ as appropriate for Wolf–Rayet progenitor stars. In this calculation, we used the bolometric luminosity we derived in M14, $E_{\rm k} \sim 10^{52}$ erg and $M_{\rm ej} \sim 3\,M_\odot$ as obtained by modeling the bolometric luminosity in M14.

The inferred limit to the mass-loss rate $\dot{M} < 5 \times 10^{-6} (M_\odot\,{\rm y}^{-1})$ is independent from any assumption on magnetic-field-related parameters; it is not affected by possible uncertainties on the SN distance and indicates that the pre-explosion mass loss of SN 2012ap lies at the low end of the interval of values derived by C14 ($4 \times 10^{-6}\,M_\odot\,{\rm y}^{-1} < \dot{M} < 5 \times 10^{-5}\,M_\odot\,{\rm y}^{-1}$) and is based on the modeling of the radio observations with synchrotron emission.[8] This result is in line with the value derived for the relativistic SN 2009bb ($\dot{M} \sim 2 \times 10^{-6}\,M_\odot\,{\rm y}^{-1}$; Soderberg et al. 2010b) and is consistent with the wide range of values inferred for sub-E GRBs ($10^{-7}\,M_\odot\,{\rm y}^{-1} \lesssim \dot{M} \lesssim 10^{-5}\,M_\odot\,{\rm y}^{-1}$).

4. SN 2012ap IN THE CONTEXT OF ENGINE-DRIVEN EXPLOSIONS

The radio observations of SN 2012ap are well modeled by synchrotron emission arising from the interaction of the SN shock with the environment (C14). C14 derive $E_k = (1.6 \pm 0.1) \times 10^{49}$ erg carried by mildly relativistic ejecta with velocity $v \sim 0.7c$ at $\delta t = 1$ d. By modeling the observed optical emission, M14 infer $E_{\rm k} \sim 10^{52}$ erg in slow moving ($v \approx 20{,}000\,{\rm km\,s}^{-1}$) material. These two values define an $E_{\rm k}$ profile significantly flatter than what was expected in the case of a pure hydrodynamical collapse ($E_{\rm k} \propto (\Gamma\beta)^{-5.2}$; e.g., Tan et al. 2001), thus pointing to the presence of an engine driving the SN 2012ap explosion (see Figure 2).

Engine-driven SNe constitute a diverse class of explosions that includes relativistic SNe, sub-E GRBs, and ordinary GRBs. SN 2012ap is intermediate between ordinary non-relativistic SNe and fully relativistic GRBs and falls into a region of the parameter space populated by sub-E GRBs and the other known relativistic SN, SN 2009bb (Figure 2).[9] With reference to Figures 3 and 4, we find the following.

1. The radio luminosity of SN 2012ap and sub-E GRBs is comparable. SN 2012ap is significantly more luminous than ordinary Ic SNe at the same epoch and even more luminous than the sub-E GRBs 100316D and 060218 (Figure 3, right panel). With $E_{\rm k} \sim 10^{52}$ erg and evidence for broad spectral features (M14), the properties of SN 2012ap in the optical band are also reminiscent of the very energetic SNe associated with sub-E GRBs and ordinary GRBs.

[8] Note that the synchrotron formalism is instead dependent on assumptions on magnetic-field-related parameters.

[9] The relativistic nature of SN 2007gr has been questioned by Soderberg et al. (2010a), and it is not included here. See, however, Paragi et al. (2010).

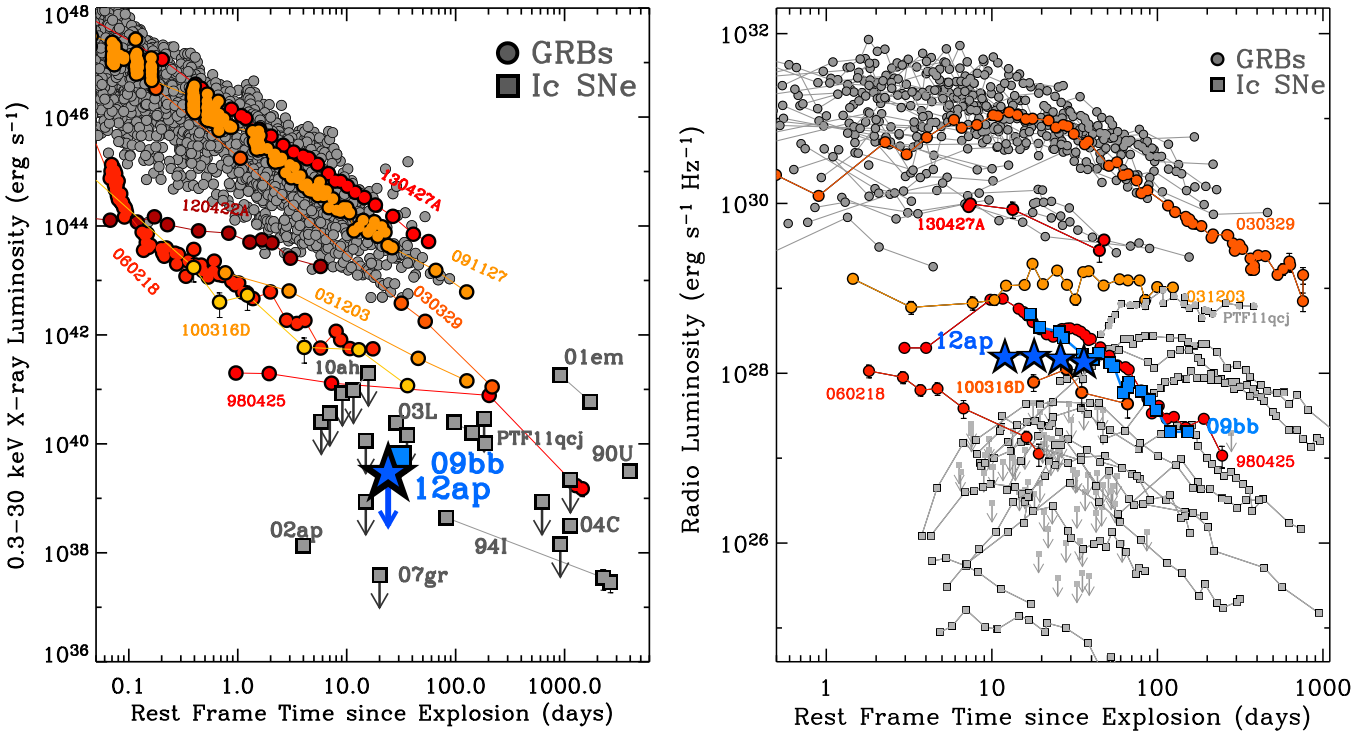

Figure 3. Left panel: *Chandra* observations put a deep limit to the X-ray luminosity of the relativistic SN 2012ap at ∼20 days after the explosion. SN 2012ap is considerably less luminous than ordinary long GRBs (filled circles; from Margutti et al. 2013a, 2013b, and references therein) and is ∼100 times fainter than the faintest sub-E GRBs (i.e., GRBs 980425 and 100316D). Filled gray squares: X-ray emission from ordinary type Ic SNe. The relativistic SN 2009bb is marked with a blue square. References: Immler et al. (2002), Pooley & Lewin (2004), Soria, Pian, & Mazzali (2004), Soderberg et al. (2005), Perna et al. (2008), Corsi et al. (2011), Horesh et al. (2013), and Corsi et al. (2014). Right panel: radio emission of SN 2012ap (from C14) compared to a sample of GRB radio afterglows (filled circles) and type Ic SNe (filled square) collected from Soderberg et al. (2010b), Corsi et al. (2011), Chandra & Frail (2012), Horesh et al. (2013), Margutti et al. (2013a), and citeCorsi14. At radio frequencies, the luminosity of SN 2012ap is comparable to (or even larger than) sub-E GRBs. In both panels, GRBs with spectroscopically associated SNe are in color and labeled. Different shades of orange and red are used to guide the eye.

(A color version of this figure is available in the online journal.)

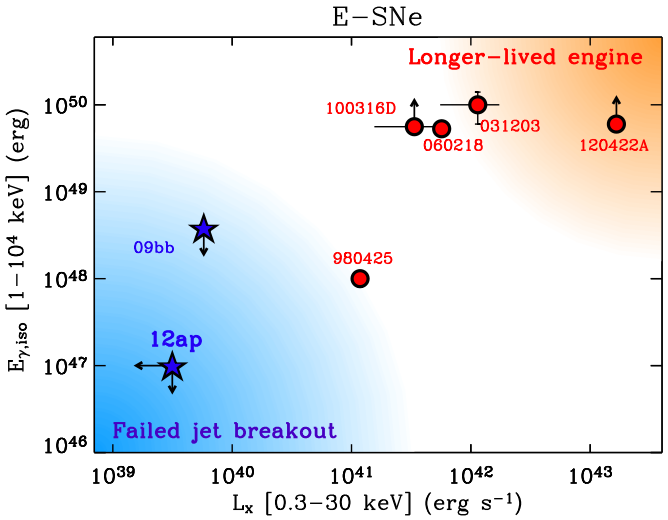

Figure 4. Promptly emitted γ-ray energy vs. X-ray luminosity between 10 and 30 days since the explosion for the sample of relativistic SNe (blue stars) and sub-E GRBs (red circles). Relativistic SNe are clearly distinguished from sub-E GRBs by their significantly fainter X-ray emission. References: Amati (2006); Soderberg et al. (2006b); Soderberg et al. (2010b); Starling et al. (2011) Barthelmy et al. (2012); Margutti et al. (2013a); Margutti et al. (2013b); Amati (2013); Amati et al. (2013); C14.

(A color version of this figure is available in the online journal.)

2. At $\delta t \sim 20$ days, the X-ray emission from SN 2012ap is, however, a factor $\geqslant$100 fainter then the faintest sub-E GRB ever detected, GRB 980425 (Figure 3, left panel).
3. Along the same line, from C14, the prompt γ-ray energy released by the SN 2012ap explosion is $E_{\gamma,\rm iso} < 10^{47}$ erg, a factor $\geqslant$10 fainter then the faintest sub-E GRB 980425 (Figure 4).

In addition, in Milisavljevic et al. (2014a) and M14, we showed the following.

1. Contrary to sub-E GRBs and GRBs, SN 2012ap exploded in a solar–metallicity environment. Interestingly, the metallicity of the environment of SN 2009bb was also super-solar (Levesque et al. 2010b).
2. Different from sub-E GRBs and GRBs, our analysis of multi-epoch spectroscopy strongly favors the presence of helium in the ejecta of SN 2012ap. Helium was also reported in the early-time spectra of SN 2009bb (Pignata et al. 2011).

Relativistic SNe and sub-E GRBs are thus clearly distinguished in terms of their high-energy (X-rays and γ-rays) properties, a higher metallicity environment, and the conspicuous presence of helium in their ejecta.

The different levels of X-ray emission between relativistic SNe and sub-E GRBs cannot be ascribed to beaming collimated emission away from our line of sight. Radio observations of sub-E GRBs support the idea of quasi-spherical explosions (e.g., Kulkarni et al. 1998; Soderberg et al. 2004, 2006a; Margutti et al. 2013a), and there is no evidence for beaming of the non-thermal emission from relativistic SNe (Soderberg et al. 2010b; C14). Furthermore, on a timescale of ∼20 days, the

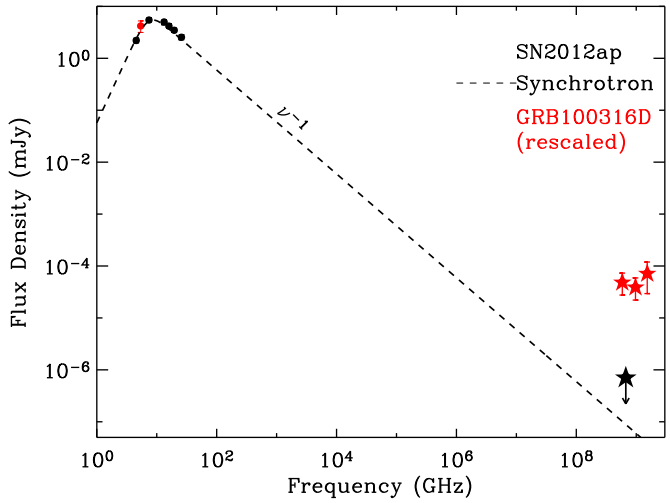

Figure 5. Radio (filled black circles) to X-ray (black stars) SED of SN 2012ap. The *Chandra* X-ray upper limit is consistent with the extrapolation of the best-fitting synchrotron model obtained by C14 at $\delta t \approx 20$ days. Notably, the X-ray emission from SN 2012ap is $\geqslant$100 times fainter than the sub-E GRB 100316D at a similar epoch (here, rescaled to match the level of the detected SN 2012ap radio emission), thus ruling out the presence of an extra X-ray component arising from the activity of the explosion central engine.

(A color version of this figure is available in the online journal.)

blastwave arising from both relativistic SNe and sub-E GRBs is sub-relativistic, and the geometry of emission is effectively spherical, independent from the initial conditions. The different levels of X-ray emission between sub-E GRBs and relativistic SNe at $t \gtrsim 10$ days are thus intrinsic.

While both relativistic SNe and sub-E GRBs are intermediate between ordinary type Ic SNe and GRBs, these findings point to a diversity in the properties of the progenitors and/or the engines that drive their explosion. This topic is discussed below.

5. DISCUSSION

At $\delta t \gtrsim 10$ days, the detected X-ray emission from sub-E GRBs like 060218 and 100316D has been suggested to originate from the activity of the explosion central engine (Soderberg et al. 2006a; Fan & Piran 2006; Fan et al. 2011; Margutti et al. 2013a), which dominates over synchrotron emission from the shock–CSM interaction.[10] The nature of the central engine is currently not known. For the sub-E GRBs 060218 and 100316D, the observations support either a magnetar central engine or continued accretion onto a newly formed black hole.

Figure 5 clearly shows that the X-ray emission from SN 2012ap is instead consistent with the shock–CSM model that best fits the radio observations. For SN 2012ap, the deep X-ray limit thus rules out the presence of an additional, luminous X-ray component arising from the engine activity, contrary to sub-E GRBs like 100316D portrayed in Figure 5. This finding suggests that the engine that powers SN 2012ap is short lived and unable to survive for such a long time.

We propose that relativistic SNe like 2009bb and 2012ap represent weak engine-driven explosions, where the engine activity stops before being able to produce a successful jet breakout. The result is a stellar explosion that is able to accelerate a tiny fraction of ejecta to mildly relativistic velocities, thus dynamically different from ordinary Ic SNe and more similar to sub-E and classical GRBs (Figure 2). In contrast to GRBs, however, the jet is not able to pierce through the stellar envelope, and a very limited fraction of energy is dissipated at γ-ray frequencies, consistent with the deep limit $E_{\gamma,\rm iso} < 10^{47}$ erg from C14. This phenomenology can either be due to an intrinsically short-lived engine or to a different progenitor structure/properties between relativistic SNe and GRBs. We discuss these two possibilities in Sections 5.1–5.3.

5.1. Central Engine Lifetime

Lazzati et al. (2012) investigated the role of the duration of the engine activity in stellar explosions induced by relativistic jets with a set of numerical simulations. These authors find that the duration of the engine activity is a key parameter that determines the outcome of a stellar explosion. For a fixed energy budget and progenitor structure, Lazzati et al. (2012) show that the longest-lived engines always produce a successful explosion with a fully relativistic jet (i.e., a classical GRB). Engines with intermediate and short durations (where "short" or "long" here refers to the time it takes to the jet head to break out through the stellar envelope) would lead instead to partially or totally failed jets, respectively. In particular, relativistic SNe would result from explosions where the engine turns off on the jet breakout timescale (5–10 s depending on the energy budget and progenitor; Morsony et al. 2007; Lazzati et al. 2012, their Figure 5), in agreement with our observational findings of shorter-lived engines.

5.2. Progenitor Properties: Metallicity

A failed jet breakout in relativistic SNe can also be due to different progenitor properties compared with sub-E GRBs and ordinary GRBs. Regarding this, it is important to note that (1) the relativistic SNe 2009bb and 2012ap exploded in super-solar and solar *metallicity* environments, respectively, in line with ordinary Ic SNe (e.g., Sanders et al. 2012a; Kelly & Kirshner 2012, and references therein) but in sharp contrast with sub-E GRBs and classical GRBs that show a marked preference for sub-solar metallicity environments (e.g., Stanek et al. 2006; Margutti et al. 2007; Modjaz et al. 2008; Levesque et al. 2010a). (2) Evidence for helium-rich ejecta was found for both SNe 2009bb (Pignata et al. 2011) and 2012ap (M14), which points to the presence of a helium layer at the time of the explosion (i.e., a not entirely envelope-stripped progenitor star).

The metallicity of the two relativistic SNe known so far is actually large even compared to the sample of energetic broad-lined Ic SNe *not* connected to GRBs and sub-E GRBs (Sanders et al. 2012a; Kelly & Kirshner 2012). For SN 2009bb, Levesque et al. (2010b) estimate $Z = 1.7$–$3.5\,Z_\odot$, while for SN 2012ap, Milisavljevic et al. (2014a) find $Z = 1.0\,Z_\odot$, where solar metallicity $Z_\odot$ corresponds to $\log(\rm O/H) + 12 = 8.69$ (Asplund et al. 2005). At such high metallicity, line-driven winds in massive stars (e.g., Castor et al. 1975) more efficiently strip away angular momentum from the progenitor through a more sustained mass loss ($\dot{M} \propto Z^{0.86}$ in Wolf–Rayet stars, likely progenitors of GRBs; Vink & de Koter 2005).[11] High angular momentum of the progenitor at collapse has been identified

[10] As noted in Margutti et al. (2013a), this extra component might be present in classical GRBs as well, but it is likely outshined by emission from the jet–CSM interaction.

[11] Recent findings indicate that episodic mass-loss episodes, as opposed to steady mass loss through winds, also have a role in the evolution of massive stars. However, the metallicity dependence of these episodes of explosive mass loss has yet to be constrained. See Margutti et al. (2014), and references therein for details.

by recent numerical simulations (e.g., MacFadyen & Woosley 1999; MacFadyen et al. 2001; Woosley & Heger 2006) as a key physical ingredient of the "collapsar" model to explain the presence of fully relativistic jets in GRBs. It is thus possible that the higher metallicity of the progenitors of relativistic SNe inhibited the formation of a powerful jet able to pierce through the stellar envelope.

The growing sample of GRBs discovered in high-metallicity environments (see, e.g., GRBs 050826 and 051022, Graham & Fruchter 2013, their Figure 3; GRB 120422A, intermediate between ordinary GRBs and sub-E GRBs, Schulze et al. 2014) points however to a more complex situation, where metallicity has some role, but it is unlikely to be the ultimate parameter driving the distribution of angular momentum at collapse.[12] These findings suggest that the higher metallicity of the two known relativistic SNe compared to GRBs might *not* be directly linked to the final explosion outcome. While it might still indicate a preference for different environments,[13] it is important to note that as opposed to GRBs and sub-E GRBs, the relativistic SNe were discovered by surveys targeting high-mass and hence metal-rich galaxies. At the time of writing, it is not clear if the higher metallicity of relativistic SNe is simply the result of this observational bias.

5.3. Progenitor Properties: Helium-rich Ejecta

The fate of a newly born jet in a massive star is also closely related to the size and structure of the progenitor star at the time of collapse, as the first requirement for a successful jet breakout is the ability to cross the progenitor and pierce through its envelope (e.g., MacFadyen & Woosley 1999; MacFadyen et al. 2001; Lazzati et al. 2012, and references therein). The detection of helium-rich ejecta in SNe 2009bb and 2012ap indicates a non-complete shredding of the outer helium layers of their progenitors before exploding, as opposed to the stripped type Ic SNe associated with GRBs and sub-E GRBs. It is thus possible that the jet failed because it was dumped by the additional helium layers of the stellar progenitors of relativistic SNe.

A similar scenario of a weak jet, dumped by the external helium layers of the stellar progenitor, was proposed for the type Ib SN 2008D by Mazzali et al. (2008) to explain the large kinetic energy ($E_k > 10^{51}$ erg), early disappearance of broad spectral features, and the serendipitous detection of a powerful X-ray flash of radiation with $L_x \sim 6 \times 10^{43}$ erg s^{-1} signaling the onset of the explosion. Later-time radio observations, however, pointed to a modest velocity of the freely expanding fastest ejecta ($\beta \approx 0.25$; Soderberg et al. 2008; Bietenholz et al. 2010). Together with the detection of strong helium lines and the disappearance of the broad spectral features, this finding clearly sets SN 2008D apart from relativistic SNe, sub-E GRBs, and GRBs (see Figure 2) and offers the case for an alternative explanation of the initial X-ray flash as shock breakout radiation from an ordinary SN (Soderberg et al. 2008).

While the nature of the X-ray flash is still under debate (e.g., Tanaka et al. 2009; Modjaz et al. 2009; van der Horst et al. 2011; Couch et al. 2011; Bersten et al. 2013; Svirski & Nakar 2014), SN 2008D brought to light the possibility that even ordinary SNe with a thicker helium envelope might be triggered by bipolar jets (Mazzali et al. 2008; Xu et al. 2008), thus pointing to a continuum of properties bridging ordinary explosions and GRBs.

5.4. A Continuum of Stellar Explosions Originating from Hydrogen-stripped Progenitors

Figure 2 strongly argues in favor of a continuum of properties of the fastest ejecta of stellar explosions originating from hydrogen-stripped progenitors (i.e., type Ib/c SNe). This finding is not new (see, e.g., Xu et al. 2008, Mazzali et al. 2008) and might be the observational manifestation of a continuum of properties of the jets that power these explosions and can potentially result from (1) different central engine lifetimes or (2) progenitor properties (i.e., metallicity or degree of stripping of the external helium layers).

While the kinetic energy profile of the ejecta E-SNe (i.e., orange, light blue, and blue dots in Figure 2) points to the presence of a central engine that drives the explosion, it is possible that even ordinary type Ib/c SNe (i.e., red dots of Figure 2) are triggered by failed bipolar jets—as opposed to the generally assumed neutrino deposition explosion mechanisms—that would leave no detectable imprint on the dynamics of the ejecta (Khokhlov et al. 1999; Granot & Ramirez-Ruiz 2004; Wheeler & Akiyama 2010; Lazzati et al. 2012; Nagakura et al. 2012).

This theoretical suggestion has been paralleled by a growing number of "transitional" objects found by recent surveys. Particularly relevant in this respect is the class of type Ic SNe with broad features in their spectra (i.e., Ic-BL, famous historical examples are SN 1997ef and SN 1997dq; Mazzali et al. 2000, 2004). While *all* E-SNe are Ic-BL, not every type Ic-BL SN showed unambiguous evidence for a central engine (Soderberg et al. 2006a, 2010b). Notable examples include the type Ic-BL SNe 2002ap (Berger et al. 2002; Gal-Yam et al. 2002; Mazzali et al. 2002), 2010ay (Sanders et al. 2012b), 2010ah (Corsi et al. 2011, Mazzali et al. 2013), and PTF10qts (Walker et al. 2014). However, persistent broad line features are found in association with large bulk kinetic energies of the ejecta ($E_k \sim 10^{52}$ erg) and are indicative of large photospheric expansion velocities that might be powered by a jet that did not emerge from the progenitor.

Finally, the growing sample of ordinary type Ib/c SNe with larger-than-average velocities of their fastest ejecta ($v \sim 0.3\,c$ versus $v \sim 0.15\,c$, as it was recently found for PTF11qcj, SN 2012au, and PTF12gzk; Corsi et al. 2014; Kamble et al. 2014; Horesh et al. 2013) further strengthens the idea of a continuum of hydrogen-stripped explosions, encompassing even ordinary SNe (Figure 2).

6. SUMMARY AND CONCLUSIONS

The class of E-SNe collects a rare variety of SN explosions ($\lesssim$1% of type Ic SNe) and includes relativistic SNe, sub-E GRBs, and ordinary GRBs. E-SNe are characterized by a significantly shallower kinetic energy profile of the explosion ejecta than expected in the case of a pure hydrodynamic collapse of the progenitor star (Figure 2), indicating that E-SNe are able to accelerate a tiny but important fraction of their ejecta to

[12] A similar conclusion is reached by studies of the close environment of GRBs and energetic broad-lined Ic SNe in the local universe. See Sanders et al. (2012a); Kelly et al. (2014).

[13] With respect to this, it is intriguing to note that for both events, the SN spectrum showed unusually strong signs of interaction with carriers of diffuse interstellar bands (DIBs) as we detail in Milisavljevic et al. (2014a). These observations suggest that the material responsible for the detected DIBs is local to the SN explosion and possibly related to the mass loss of the progenitor star in the decades to years before the terminal explosion. Alternatively, it could point to a peculiar small-scale environment in which the progenitors of relativistic SNe preferentially form.

higher velocities ($v \gtrsim 0.6\,c$). E-SNe otherwise show a diverse phenomenology.

Relativistic SNe and sub-E GRBs share a bright radio emission and evidence for mildly relativistic ejecta that clearly set them apart from ordinary SNe Ic (non-relativistic). The thermal properties of relativistic SNe are also analogous to the very energetic, fast expanding SNe associated with sub-E GRBs and ordinary GRBs (Soderberg et al. 2010b; M14). However, a distinctive property of relativistic SNe is their significantly fainter X-ray emission (Figure 3) that implies the lack of a luminous X-ray components arising from the central engine activity at late times ($\delta t \sim 20$ days; Figure 5). With $E_{\gamma,\rm iso} < 10^{47}$ erg, the prompt γ-ray energy released by the relativistic SN 2012ap is also considerably below the level of sub-E GRBs (Figure 4).[14] The higher metallicity of the environment and the conspicuous presence of helium in the ejecta of the two known relativistic SNe also sets them apart from sub-E GRBs and GRBs.

These findings call for some crucial diversity in the properties of the engines and/or of the progenitors of relativistic SNe and sub-E GRBs (and ordinary GRBs as well). We showed that the observations of relativistic SNe are consistent with the picture of jet-driven explosions where the jet just barely fails to break out from the progenitor star. This scenario naturally explains (1) the lack of evidence for central engine activity at late times and (2) the deep limit to the promptly released γ-ray energy.

The failed jet breakout might be due to an intrinsically short-lived engine (but the same progenitor properties) or to a different progenitor structure between relativistic SNe and sub-E GRBs. At the time of writing, with only two relativistic SNe discovered so far (through targeted optical surveys), observations do not allow us to distinguish between these two scenarios. A significantly larger sample of relativistic SNe found through *untargeted* SN searches in the optical and radio band is clearly needed to deeply understand their connection to GRBs, build a complete picture of E-SNe, and constrain which unique property differentiates failed breakouts from successful, fully relativistic jets. The Large Synoptic Survey Telescope (Ivezic et al. 2008) is expected to discover hundreds of SNe Ic every year, thus, in principle, providing the significantly larger sample of E-SNe that is needed to deeply understand the connection between relativistic SNe and GRBs. However, as we demonstrate here, coordinated radio and X-ray follow-up is essential to identify E-SNe from their ordinary counterparts and determine the properties of the engines that power their explosion.

We thank the referee for useful comments and suggestions that improved the quality of our paper. R.M. is grateful to the Aspen Center for Physics and NSF grant 1066293 for hospitality during the completion of this work. Support for this work was provided by the David and Lucile Packard Foundation Fellowship for Science and Engineering awarded to A.M.S.

[14] For the other relativistic SN 2009bb, the observational limit on the promptly released $E_{\gamma,\rm iso}$ is unfortunately not as constraining (Figure 4).

REFERENCES

Amati, L. 2006, MNRAS, 372, 233
Amati, L. 2013, AstRv, 8, 010000
Amati, L., Dichiara, S., Frontera, F., & Guidorzi, C. 2013, GCN, 14503, 1
Asplund, M., Grevesse, N., & Sauval, A. J. 2005, in ASP Conf. Ser. 336, Cosmic Abundances as Records of Stellar Evolution and Nucleosynthesis, ed. T. G. Barnes, III & F. N. Bash (San Francisco, CA: ASP), 25
Barthelmy, S. D., Baumgartner, W. H., Cummings, J. R., et al. 2012, GCN, 13246, 1
Ben-Ami, S., Gal-Yam, A., Filippenko, A. V., et al. 2012, ApJL, 760, L33
Berger, E., Kulkarni, S. R., & Chevalier, R. A. 2002, ApJL, 577, L5
Berger, E., Kulkarni, S. R., Frail, D. A., & Soderberg, A. M. 2003, ApJ, 599, 408
Bersten, M. C., Tanaka, M., Tominaga, N., Benvenuto, O. G., & Nomoto, K. 2013, ApJ, 767, 143
Bietenholz, M. F., Soderberg, A. M., Bartel, N., et al. 2010, ApJ, 725, 4
Björnsson, C.-I., & Fransson, C. 2004, ApJ, 605, 823
Bromberg, O., Nakar, E., & Piran, T. 2011, ApJL, 739, L55
Burrows, D. N., Hill, J. E., Nousek, J. A., et al. 2005, SSRv, 120, 165
Campana, S., Mangano, V., Blustin, A. J., et al. 2006, Natur, 442, 1008
Castor, J. I., Abbott, D. C., & Klein, R. I. 1975, ApJ, 195, 157
Chakraborti, S., & Ray, A. 2011, ApJ, 729, 57
Chakraborti, S., Ray, A., Soderberg, A. M., Loeb, A., & Chandra, P. 2011, NatCo, 2, 175
Chakraborti, S., Soderberg, A., Chomiuk, L., et al. 2014, arXiv:1402.6336
Chandra, P., & Frail, D. A. 2012, ApJ, 746, 156
Chevalier, R. A., & Fransson, C. 2006, ApJ, 651, 381
Cobb, B. E., Bailyn, C. D., van Dokkum, P. G., & Natarajan, P. 2006, ApJL, 645, L113
Corsi, A., Ofek, E. O., Frail, D. A., et al. 2011, ApJ, 741, 76
Corsi, A., Ofek, E. O., Gal-Yam, A., et al. 2014, ApJ, 782, 42
Couch, S. M., Pooley, D., Wheeler, J. C., & Milosavljević, M. 2011, ApJ, 727, 104
Coward, D. M. 2005, MNRAS, 360, L77
Dessart, L., Burrows, A., Livne, E., & Ott, C. D. 2008, ApJL, 673, L43
Fan, Y., & Piran, T. 2006, MNRAS, 369, 197
Fan, Y.-Z., Zhang, B.-B., Xu, D., Liang, E.-W., & Zhang, B. 2011, ApJ, 726, 32
Filippenko, A. V. 1997, ARA&A, 35, 309
Gal-Yam, A., Ofek, E. O., & Shemmer, O. 2002, MNRAS, 332, L73
Gehrels, N., Chincarini, G., Giommi, P., et al. 2004, ApJ, 611, 1005
Graham, J. F., & Fruchter, A. S. 2013, ApJ, 774, 119
Granot, J., & Ramirez-Ruiz, E. 2004, ApJL, 609, L9
Guetta, D., & Della Valle, M. 2007, ApJL, 657, L73
Horesh, A., Kulkarni, S. R., Corsi, A., et al. 2013, ApJ, 778, 63
Immler, S., Wilson, A. S., & Terashima, Y. 2002, ApJL, 573, L27
Ivezic, Z., Axelrod, T., Brandt, W. N., et al. 2008, SerAJ, 176, 1
Kalberla, P. M. W., Burton, W. B., Hartmann, D., et al. 2005, A&A, 440, 775
Kamble, A., Soderberg, A. M., Chomiuk, L., et al. 2014, ApJ, 797, 2
Katz, B., Budnik, R., & Waxman, E. 2010, ApJ, 716, 781
Kelly, P. L., Filippenko, A. V., Modjaz, M., & Kocevski, D. 2014, ApJ, 789, 23
Kelly, P. L., & Kirshner, R. P. 2012, ApJ, 759, 107
Khokhlov, A. M., Höflich, P. A., Oran, E. S., et al. 1999, ApJL, 524, L107
Kulkarni, S. R., Frail, D. A., Wieringa, M. H., et al. 1998, Natur, 395, 663
Lazzati, D., Morsony, B. J., Blackwell, C. H., & Begelman, M. C. 2012, ApJ, 750, 68
Levesque, E. M., Kewley, L. J., Berger, E., & Zahid, H. J. 2010a, AJ, 140, 1557
Levesque, E. M., Soderberg, A. M., Foley, R. J., et al. 2010b, ApJL, 709, L26
Liang, E., Zhang, B., Virgili, F., & Dai, Z. G. 2007, ApJ, 662, 1111
MacFadyen, A. I., & Woosley, S. E. 1999, ApJ, 524, 262
MacFadyen, A. I., Woosley, S. E., & Heger, A. 2001, ApJ, 550, 410
Margutti, R., Chincarini, G., Covino, S., et al. 2007, A&A, 474, 815
Margutti, R., Milisavljevic, D., Soderberg, A. M., et al. 2014, ApJ, 780, 21
Margutti, R., Soderberg, A. M., Chomiuk, L., et al. 2012, ApJ, 751, 134
Margutti, R., Soderberg, A. M., Wieringa, M. H., et al. 2013a, ApJ, 778, 18
Margutti, R., Zaninoni, E., Bernardini, M. G., et al. 2013b, MNRAS, 428, 729
Matzner, C. D., & McKee, C. F. 1999, ApJ, 510, 379
Mazzali, P. A., Deng, J., Maeda, K., et al. 2002, ApJL, 572, L61
Mazzali, P. A., Deng, J., Maeda, K., et al. 2004, ApJ, 614, 858
Mazzali, P. A., Iwamoto, K., & Nomoto, K. 2000, ApJ, 545, 407
Mazzali, P. A., Valenti, S., Della Valle, M., et al. 2008, Sci, 321, 1185
Mazzali, P. A., Walker, E. S., Pian, E., et al. 2013, MNRAS, 432, 2463
Milisavljevic, D., Margutti, R., Crabtree, K. N., et al. 2014a, ApJL, 782, L5
Milisavljevic, D., Margutti, R., Parrent, J. T., et al. 2014b, ApJ, in press (arXiv:1408.1606)
Modjaz, M., Kewley, L., Kirshner, R. P., et al. 2008, AJ, 135, 1136
Modjaz, M., Li, W., Butler, N., et al. 2009, ApJ, 702, 226
Morsony, B. J., Lazzati, D., & Begelman, M. C. 2007, ApJ, 665, 569
Nagakura, H., Suwa, Y., & Ioka, K. 2012, ApJ, 754, 85
Nakar, E., & Sari, R. 2012, ApJ, 747, 88
Paragi, Z., Taylor, G. B., Kouveliotou, C., et al. 2010, Natur, 463, 516
Perna, R., Soria, R., Pooley, D., & Stella, L. 2008, MNRAS, 384, 1638
Pian, E., Mazzali, P. A., Masetti, N., et al. 2006, Natur, 442, 1011
Pignata, G., Stritzinger, M., Soderberg, A., et al. 2011, ApJ, 728, 14

Pooley, D., & Lewin, W. H. G. 2004, IAU Circ., 8323, 2
Predehl, P., & Schmitt, J. H. M. M. 1995, A&A, 293, 889
Sanders, N. E., Soderberg, A. M., Levesque, E. M., et al. 2012a, ApJ, 758, 132
Sanders, N. E., Soderberg, A. M., Valenti, S., et al. 2012b, ApJ, 756, 184
Schulze, S., Malesani, D., Cucchiara, A., et al. 2014, A&A, 566, 102
Soderberg, A. M., Berger, E., Kasliwal, M., et al. 2006a, ApJ, 650, 261
Soderberg, A. M., Berger, E., Page, K. L., et al. 2008, Natur, 453, 469
Soderberg, A. M., Brunthaler, A., Nakar, E., Chevalier, R. A., & Bietenholz, M. F. 2010a, ApJ, 725, 922
Soderberg, A. M., Chakraborti, S., Pignata, G., et al. 2010b, Natur, 463, 513
Soderberg, A. M., Kulkarni, S. R., Berger, E., et al. 2004, Natur, 430, 648
Soderberg, A. M., Kulkarni, S. R., Berger, E., et al. 2005, ApJ, 621, 908
Soderberg, A. M., Kulkarni, S. R., Nakar, E., et al. 2006b, Natur, 442, 1014
Soria, R., Pian, E., & Mazzali, P. A. 2004, A&A, 413, 107
Springob, C. M., Masters, K. L., Haynes, M. P., Giovanelli, R., & Marinoni, C. 2007, ApJS, 172, 599
Springob, C. M., Masters, K. L., Haynes, M. P., Giovanelli, R., & Marinoni, C. 2009, ApJS, 182, 474
Stanek, K. Z., Gnedin, O. Y., Beacom, J. F., et al. 2006, AcA, 56, 333
Starling, R. L. C., Wiersema, K., Levan, A. J., et al. 2011, MNRAS, 411, 2792
Svirski, G., & Nakar, E. 2014, ApJL, 788, L14
Tan, J. C., Matzner, C. D., & McKee, C. F. 2001, ApJ, 551, 946
Tanaka, M., Yamanaka, M., Maeda, K., et al. 2009, ApJ, 700, 1680
van der Horst, A. J., Kamble, A. P., Paragi, Z., et al. 2011, ApJ, 726, 99
Vink, J. S., & de Koter, A. 2005, A&A, 442, 587
Virgili, F. J., Liang, E.-W., & Zhang, B. 2009, MNRAS, 392, 91
Walker, E. S., Mazzali, P. A., Pian, E., et al. 2014, MNRAS, 442, 2768
Wang, X.-Y., Li, Z., Waxman, E., & Mészáros, P. 2007, ApJ, 664, 1026
Watson, D. 2011, A&A, 533, A16
Waxman, E., Mészáros, P., & Campana, S. 2007, ApJ, 667, 351
Wheeler, J. C., & Akiyama, S. 2010, NewA, 54, 183
Woosley, S. E., & Heger, A. 2006, ApJ, 637, 914
Xu, D., Watson, D., Fynbo, J., et al. 2008, 37th COSPAR Assembly, 3512